Performance Evaluation of Graphene Nanoribbon Infrared Photodetectors

M. Pourfath, O. Baumgartner, H. Kosina, and S. Selberherr
Institute for Microelectronics, TU Wien, 1040 Vienna, Austria
Email: {pourfath|baumgartner|kosina|selberherr}@iue.tuwien.ac.at

***Abstract*—Graphene nanoribbons have recently attracted much interest as they are recognized as promising building blocks for nanoelectronic devices. The direct bandgap and the tunability of the relatively narrow bandgap with the ribbon's width renders them as suitable candidates for opto-electronic devices, especially for infrared applications. The performance of infrared photo detectors based on graphene nanoribbons is analyzed numerically, employing the non-equilibrium Green's function formalism.**

I. Introduction

Graphene has been extensively studied in recent years due to its exceptional electronic, opto-electronic, and mechanical properties [1]. This material shows an extraordinarily high carrier mobility of more than 2×10^5 $\mathrm{cm}^2/\mathrm{Vs}$ [2] and is considered to be a major candidate for future high speed transistor materials. One of the many interesting properties of Dirac electrons in graphene are the drastic changes of the conductivity of graphene-based structures with the confinement of electrons. Structures based on graphene realizing this behavior are *carbon nanotubes* (CNTs) and *graphene nanoribbons* (GNRs) with, respectively, periodic and zero boundary conditions for the transverse electron wavevector. The limited control over chirality and diameter of the nanotubes and thus of the associated electronic bandgap remains a major technological problem. A further limitation is the requirement for sufficiently tightly packed arrays of nanotubes to achieve electrical current levels comparable to Si-FETs [3].

Recently, graphene sheets have been patterned into narrow nanoribbons [4] and GNRs have attracted particular interest as they are recognized as promising building blocks for nanoelectronic devices [5]. The electronic properties of GNRs exhibit a dependence on the ribbon direction and width. In principle, GNRs can be patterned directly into device structures and even into integrated circuits by a single patterning process of a graphene sheet, as has been demonstrated by recent experiments [6]. Moreover, owing to excellent optical properties, an all graphene nanoribbon electronic and opto-electronic circuit can be envisioned. To explore the physics of such devices quantum mechanical simulations have been performed, employing the non-equilibrium Green's function formalism (NEGF). We employed the NEGF method along with a tight-binding model to study quantum transport in infrared (IR) photo detectors based on graphene nanoribbons.

II. Non-equilibrium Green's Function Formalism

The NEGF formalism initiated by Schwinger, Kadanoff, and Baym allows to study the time evolution of a many-particle quantum system. Knowing the single-particle Green's functions of a given system, one may evaluate single-particle quantities such as carrier concentration and current density. The many-particle information about the system is cast into self-energies which are part of the equations of motion for the Green's functions. Green's functions enable a powerful technique to evaluate the properties of a many-body system both in thermodynamic equilibrium and non-equilibrium situations.

Four types of Green's functions are defined as the non-equilibrium statistical ensemble averages of the single particle correlation operator. The greater Green's function $G^{>}$ and the lesser Green's function $G^{<}$ deal with the statistics of carriers. The retarded Green's function G^{R} and the advanced Green's function G^{A} describe the dynamics of carriers.

In steady-state condition the equation of motion for the Green's functions can be written as:

$$[E - H_0]\, G^{\mathrm{R,A}}(1,2) - \int d3\ \Sigma^{\mathrm{R,A}}(1,3) G^{\mathrm{r,a}}(3,2) = \delta_{1,2}$$

$$G^{\lessgtr}(1,2) = \int d3 \int d4\ G^{\mathrm{R}}(1,3) \Sigma^{\lessgtr}(3,4) G^{\mathrm{A}}(4,2)$$

The abbreviation $1 \equiv (\mathbf{r_1}, t_1)$ is here adopted. H_0 is the single-particle Hamiltonian operator, and Σ^{R}, Σ^{A}, $\Sigma^{<}$, and $\Sigma^{>}$ are the retarded, advanced, lesser, and greater self-energies, respectively.

III. Implementation

A tight-binding Hamiltonian is used to describe transport phenomena in a $(12,0)$ armchair GNR. In graphene three σ bonds hybridize in an sp^2 configuration, whereas the other $2p_z$ orbital, which is perpendicular to the graphene layer, forms π covalent bonds. The π energy bands are predominantly determining the solid state properties of graphene. Similar considerations hold for CNTs. We use a nearest-neighbor tight-binding π-bond model [7]. Each atom in an sp^2-coordinated CNT has three nearest neighbors, located $a_{\mathrm{cc}} = 1.42$ Å away. The bandstructure consists of π-orbitals only, with the hopping parameter $t = V_{pp\pi} \approx -2.7$ eV and zero on-site potential.

The Hamiltonian of the electron-photon interaction can be written as [8, 9]:

$$\hat{H}_{e-ph} = \sum_{l,m} M_{l,m} \left(\hat{b} e^{-i\omega t} + \hat{b}^{\dagger} e^{+i\omega t} \right) \hat{a}_l^{\dagger} \hat{a}_m \qquad (1)$$

$$M_{l,m} = (r_m - r_l)\, \frac{i\mathrm{e}}{\hbar} \sqrt{\frac{\hbar I_\omega}{2N\omega\epsilon c}} \langle l | \hat{H}_0 | m \rangle \qquad (2)$$

r_m denotes the position of the carbon atom at site m, I_ω is the flux of photons with the frequency ω, and N is the photon number in the control volume. The incident light is assumed to be monochromatic, with polarization along the

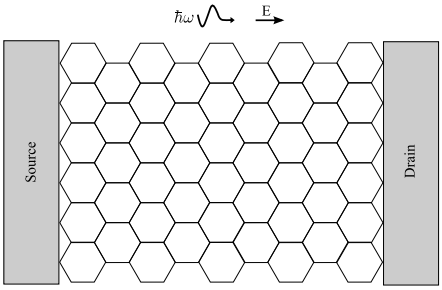

Fig. 1. The sketch of an $(12, 0)$ armchair GNR based photodetector. Incident photons generate electron-hole pairs and the electric field drives electrons and holes towards the drain and source contacts, respectively.

GNR length, see Fig. 1. We employed the lowest order self-energy of the electron-photon interaction [10]. The transport equations must be iterated to achieve convergence of the electron-photon self-energies, resulting in a self-consistent Born approximation [11].

IV. Results

Fig. 2 shows the density of states of an $(12, 0)$ armchair GNR for the first three subbands. Van-hove singularities in the density of states result in large photon-assisted transitions from the valence to the conduction band [12]. Some of the most important transitions are marked.

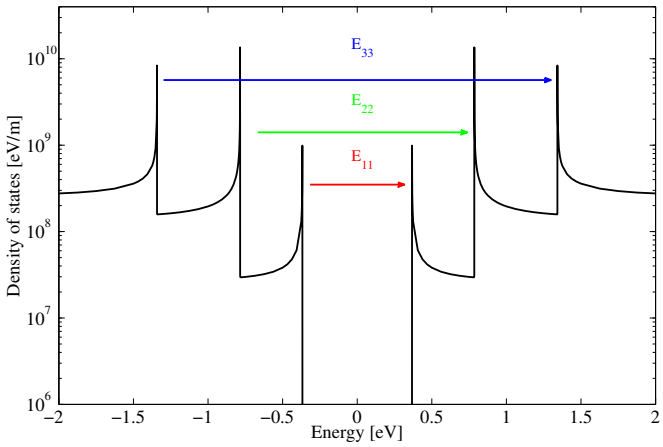

Fig. 2. The density of states of an $(12, 0)$ armchair GNR. Some of the most important transitions are marked: E_{ij} denotes a transition from the ith valence band to the jth conduction band.

To investigate GNR photodetectors we study the quantum efficiency which is defined as:

$$\alpha = \frac{I_{\rm ph}/q0}{P_{\rm op}/\hbar\omega} \tag{3}$$

$I_{\rm ph}$ is the photo current and $P_{\rm op}$ is the incident optical power. This quantity corresponds in fact to the energy conversion efficiency of a photodetector. Fig. 3 shows the calculated quantum efficiency of the investigated device as a function of the incident photon energy. The efficiency is maximized, when the photon energy matches the bandgap of the GNR. The maximum quantum efficiency ranges from 9% to 11% and is fairly independent of the bandgap [9]. An experimental and a theoretical study of CNT based photodetectors has estimated a quantum efficiency in the $10 - 20\%$ range [9, 13]. Due to periodic boundary conditions the subbands of CNTs appear as double degenerate. However, in GNRs this symmetry is removed and subbands are no longer degenerate. As a result the current capacity in GNRs is roughly half of that of their CNT counterparts. It is, therefore, reasonable to expect a maximum quantum efficiency of 10% in GNR devices.

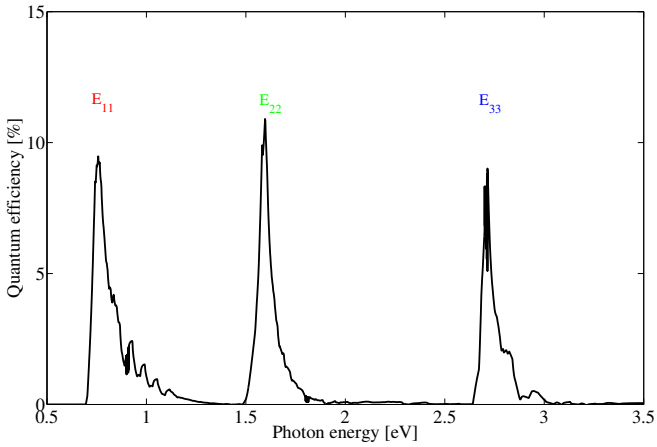

Fig. 3. The calculated quantum efficiency as a function of the incident photon energy.

Another figure of merit which is of interest for photodetectors is the photo-responsivity given by $I_{\rm ph}/P_{\rm op}$. Our calculations give an upper limit for the responsivity of 0.15 A/W for photon energies near the GNR band gap, which is nearly half of that of CNTs [9].

V. Conclusion

We present a study of GNR-based photo-detectors employing the NEGF method. The results indicate a clear prove of using GNRs for future photodetectors. Due to the removal of band-degeneracy photo-current in GNR devices is roughly half of that of their CNT counterparts. Although CNT photodetectors show better performance, the fabrication of GNRs is more compatible with current semiconductor technologies, which renders them well suitable for future optoelectronic applications.

VI. Acknowledgments

This work, as part of the European Science Foundation EUROCORES Programme FoNE, was partly supported by funds from FWF (Contract I79-N16).

References

[1] J. Appenzeller, Proc. IEEE **96**, 201 (2008).
[2] X. Du *et al.*, Nature Nanotech. **3**, 491 (2008).
[3] D. Akinwande *et al.*, IEEE Trans. Nanotechnol. **5**, 599 (2006).
[4] C. Berger *et al.*, Science **312**, 1191 (2006).
[5] M. Freitag, Nature Nanotech. **3**, 455 (2008).
[6] Z. Chen *et al.*, arXiv:cond-mat/0701599 (2007).
[7] D. Finkenstadt *et al.*, Phys. Rev. B **76**, 121405 (4pp) (2007).
[8] L. E. Henrickson, J. Appl. Phys. **91**, 6273 (2002).
[9] D. A. Stewart *et al.*, Phys. Rev. Lett. **93**, 107401 (2004).
[10] R. Lake *et al.*, J. Appl. Phys. **81**, 7845 (1997).
[11] S. Datta, Superlattices Microstruct. **28**, 253 (2000).
[12] H. Hsu *et al.*, Phys. Rev. B **76**, 045418 (5pp) (2007).
[13] M. Freitag *et al.*, Nano Lett. **3**, 1067 (2003).